

Wonderful Matrices: More Efficient and Effective Architecture for Language Modeling Tasks

Jingze Shi^{*1}, Bingheng Wu^{†2}, Lu He^{†3}, and Luchang Jiang^{†4}

Independent Researcher

losercheems@gmail.com

wubingheng52136@gmail.com, 2196187034@qq.com, auroral.sunflower@gmail.com

Abstract

We prove the availability of inner product form position encoding in the state space duality algorithm and study the effectiveness of different position embeddings in the hybrid quadratic causal self-attention and state space duality algorithms. We propose inner function attention with dynamic mask, which can improve the expressiveness of the attention algorithm and avoid the sequence noise significantly affecting the accuracy of the attention score. We also design cross domain mixture of experts, which can improve the granularity of the sparse activation feedforward network while maintaining the efficiency of parameter utilization and retrieval. The combination of these methods constitutes our foundation model architecture: Wonderful Matrices. We conduct experiments on the language modeling task and find that Wonderful Matrices are more efficient and effective in handling complex language tasks.

1 Introduction

Efficient algorithms aim to compress information in a limited state so that it can store as much useful information as possible in a limited state space, while effective algorithms aim to store all information states and build dependencies between information to avoid capturing biased information.

Transformers (Vaswani et al. 2017) Architecture is popular in modern deep learning language modeling, which can directly capture the relationship between any two elements in the sequence and effectively deal with long-distance dependency problems. However, the architecture has two main drawbacks. First, when dealing with long sequences, the quadratic complexity of its causal self-attention algorithm and the cache size limit the ability to process long contexts. Second, Transformers lack a single summary state, which means that each generated token must be computed over the entire context.

Concurrently with this, the State Space Model (Mamba2 (Dao and Gu 2024)) came into being. Mamba2 stores effective relevant information through its selective state update algorithm, balances the quadratic and linear calculation methods (state space duality) of relevant matrices, achieves linear scaling of sequence length during training, and maintains a constant state size during generation. In addition, due to its linear recursive state update mechanism, Mamba2 has a single summary state. However, Mamba2 also has a major drawback: its state does not expand with the sequence length, and information compression inevitably leads to information loss.

To build a model that is both efficient and effective, the key is to balance the relationship between compressing information states and storing all information states. Our main goal is to integrate the state space duality(referred to as SSD in the following) algorithm with the quadratic causal self-attention(referred to as QCAtn in the following) algorithm to overcome their respective limitations. Although this hybrid algorithm foundation model architecture will lose some of the extreme excellence of a single algorithm in a specific task, it will have the comprehensive ability of information filtering, long-term dependencies in long contexts, summary states, efficient learning, and low memory usage. This paper aims to further explore how to combine the selective state space algorithm with the quadratic self-attention algorithm,

^{*}Algorithm Design and Experiment Verification.

[†]Feature Analysis and Datasets Processing.

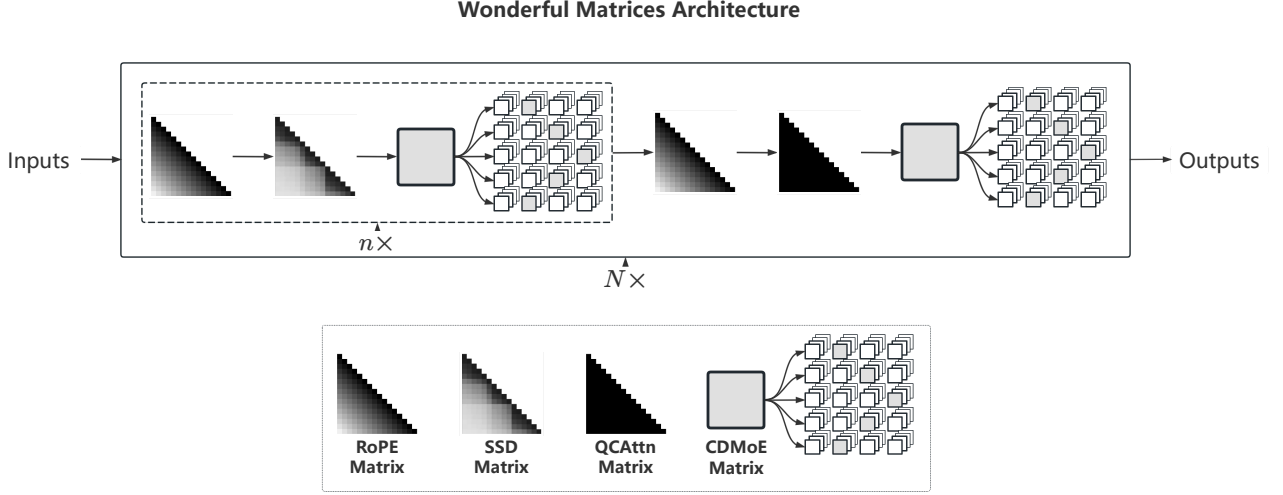


Figure 1: **Wonderful Matrices Architecture**. Shows the matrices used in the Wonderful Matrices architecture, including the rotary position embedding matrix, state space duality matrix, quadratic causal self-attention matrix, cross domain mixture of experts matrix, and the process of using these matrices. The specific structure and algorithm of these matrices will be detailed in subsequent chapters.

and cooperate with the mixture of experts with cross-domain general knowledge to build a foundation model architecture that is more comprehensive than Transformers or Mamba.

Position Encoding. The key to combining the SSD algorithm with the QCAtn algorithm is the effective integration of positional information. In Mamba (Gu and Dao 2023), the position information is implicitly provided by causal convolution, and matrix D is used to skip the connection to the input and output of the selective state space algorithm, re-continuing the discrete positional information. In Mamba2 (Dao and Gu 2024), the cumulative product is proposed to allow two positions to interact, which is a form of relative positional embedding. However, additional convolution operations for position encoding are time-consuming, and recursive position encoding is only applicable to the SSD algorithm and cannot be applied to QCAtn. We need a unified position encoding to ensure the consistency of positional information in the two algorithms. We have proven the availability of rotary position embedding in the SSD algorithm to ensure the consistency of positional information in the two algorithms.

Algorithm Mixing. Improving the efficiency of sequence transformation requires reducing the proportion of QCAtn in the entire sequence transformation layer, and to maintain the effectiveness of sequence transformation, we need to increase the expressive power of QCAtn. Grouped-query attention (Ainslie et al. 2023) found that by corresponding multiple queries to a group of keys and values, there is only a slight quality degradation compared to multi-head attention, but a significant reduction in memory bandwidth for loading keys and values. Conversely, increasing the expressiveness of values will improve the quality of modeling, but we cannot simply increase the number of values to sacrifice efficiency for effect, which contradicts the original intention of GQA. We propose the inner function attention and dynamic attention mask method, which modifies the Value in QCAtn from a linear mapping to the input to a heuristic function that can store more information, and prevents excessive information noise from affecting the calculation of the attention score matrix.

Cross Domain. The effectiveness of state transformation lies in the match between its structure and the data to be learned. In human society, knowledge is widely distributed in different domains, which are interconnected through common general knowledge and cross domain knowledge. We design cross domain mixture of experts (referred to as CDMoE in the following), which has shared parameters for storing general knowledge and professional parameters for storing domain-specific knowledge, and the professional parameters are shared within a certain range to meet the needs of cross

domain knowledge learning. And CDMoE can significantly improve the granularity of experts without causing a rapid decline in computational speed.

Architecture Design. We use the rotary position embedding matrix as the position encoding method for the state space duality matrix and the quadratic causal self-attention matrix. Considering that the quadratic causal self-attention is slow in long sequence calculations, in order to extend the model depth, multiple state space duality matrices are used before it. After the sequence transformation of each state space duality matrix or quadratic causal self-attention matrix, the cross domain mixture of experts matrix is used for state transformation. These matrices form the Wonderful Matrices architecture, as shown in Figure 1.

We empirically evaluate the Wonderful Matrices architecture on the language modeling task, including the improvement verification of specific modules and the verification of the overall architecture. These experiments demonstrate the efficiency and effectiveness of the Wonderful Matrices architecture in handling complex language tasks.

2 Related Work

Quadratic Causal Self-Attention. Self-Attention is a mechanism that computes the relevance scores between each element in the sequence and all other elements, allowing each element to "attend" to other elements. The most important variant of attention is the quadratic self-attention.

$$Y = \text{softmax}(QK^T) \cdot V$$

A notable feature of quadratic self-attention is that it can capture dependencies between any positions in the input sequence, without being limited by distance, and the state expands with the sequence length, which gives it an advantage in capturing long-range dependencies in long sequences.

In causal language modeling, a causal mask is usually added to it, which We will refer to as QCAtn (Quadratic Causal Self-Attention) in the following.

State Space Duality. Many variants of attention have been proposed, all of which are based on the core of attention scores.

linear attention (Katharopoulos et al. 2020) discards softmax by folding it into the kernel feature map and rewrites $(QK^T) \cdot V = Q \cdot (K^T V)$ using the kernel property of matrix multiplication. In the case of causal (autoregressive) attention, they show that when the causal mask is merged to the left as $(L \circ QK^T) \cdot V$, where L is a lower triangular matrix, the right side can be expanded into a recursive form.

In Transformers are SSMs (Dao and Gu 2024), the SSD (State Space Dual) is used to prove that simply computing the scalar structured SSM — by materializing the semi-separable matrix $M = L \circ CB^T = L \circ QK^T$ and performing quadratic matrix-vector multiplication — is equivalent to quadratic masked kernel attention.

$$(L \circ QK^T) \cdot V = (L \circ CB^T) \cdot X$$

Positional Encoding. Position information is important in language modeling, and there are mainly three forms of relative positional encoding: convolution, recursive, and inner product.

The source of positional information in Mamba (Gu and Dao 2023) is causal convolution and matrix D that skips the connection between input and output.

In Mamba2 (Dao and Gu 2024), element a_t acts as a "gate" or "selector", and its cumulative product $a_{(j : i)}$ controls the amount of interaction allowed between position i and position j , which can be seen as a form of relative positional embedding.

RoPE (Su et al. 2021) adds absolute positional information to Q and K in self-attention, and obtains the relative positional encoding matrix $[B, L, L]$ by calculating the inner product of $QK^T [B, L, D] \times [B, L, D]^T$.

Mixture of Experts. The sparse activation mixture of experts architecture aims to train a larger model in fewer training steps with limited computational resources, which often performs better than training a smaller model in more steps.

In the routing expert strategy, to ensure that the experts learn non-redundant general knowledge, shared expert isolation (Dai et al. 2024)(referred to as SEI in the following) shares knowledge by isolating k experts, adding the entire sequence state of the isolated experts to the state of each token of the routing expert to ensure that the experts learn non-redundant general knowledge.

Mixture of A Million Experts. The finer the granularity of the sparse activation mixture of experts, the better the performance. Mixture of A Million Experts (He 2024) proposes PEER (parameter efficient expert retrieval) to maintain computational efficiency under a large number of experts.

Expressive Hidden States. Learning to (Learn at Test Time) (Sun et al. 2024) proposes to make the hidden state the machine learning model itself to increase its expressive power. The hidden state is a neural network that can be trained to perform any task, and the model can be trained to learn the hidden state.

3 Methods

Wonderful Matrices is a foundation architecture designed to build efficient and effective models.

Rotary Position Embedding for Hybrid Algorithms. When mixing SSD with QCAtn algorithms, we have proven the availability of the rotary position embedding matrix in the hybrid algorithm. The method is described in Section 3.1.

Inner Function Attention with Dynamic Attention Mask. We propose inner function attention to store more shared value states, and cooperate with dynamic attention mask to ensure the accuracy of attention scores. The method is described in Section 3.2.

Cross Domain Mixture of Experts. We propose CDMoE. The ratio of shared parameters to private parameters can be adjusted arbitrarily, and compared with the classic routing mixture of experts, it expands the number of experts significantly without causing a decrease in expert retrieval speed. The method is described in Section 3.3.

Architecture Design. We combine these methods to design the Wonderful Matrices architecture. The architecture is described in Section 3.4.

3.1 Rotary Position Embedding for Hybrid Algorithms

For example, in the self-attention QK^\top , the dot product of two vectors $Q_i \cdot K_j$ is calculated, and the result is a scalar, which represents the correlation between position i and position j .

Dot Product Rotary Position The basic idea of rotary position embedding is to encode the position information as a complex rotary matrix, whose angle is determined by the position index. When QK or CB is applied with RoPE, if an element position is close to the front, its rotary will affect the direction of the K or B vector multiplied by it, thereby affecting the result of the inner product.

Define RoPE as $f_{\{Q,K\}}(x_i, i)$ and $f_{\{C,B\}}(x_i, i)$, where x_i is the input vector, and i is the position index, then:

$$f_{\{Q,K\}}(x_i, i) = \mathbb{R}_{\Theta, i}^d W_{\{Q,K\}} x_i \quad (1)$$

$$f_{\{C,B\}}(x_i, i) = \mathbb{R}_{\Theta, i}^d W_{\{C,B\}} x_i \quad (2)$$

where Θ and $\mathbb{R}_{\Theta, i}^d$ are defined as follows:

$$\Theta = \{\theta_i = n^{-2(i-1)/d}, i \in [1, 2, \dots, d/2]\} \quad \mathbb{R}_{\Theta, i}^d = \begin{bmatrix} \cos i\theta_0 & -\sin i\theta_0 & 0 & 0 & \dots & 0 & 0 \\ \sin i\theta_0 & \cos i\theta_0 & 0 & 0 & \dots & 0 & 0 \\ 0 & 0 & \cos i\theta_1 & -\sin i\theta_1 & \dots & 0 & 0 \\ 0 & 0 & \sin i\theta_1 & \cos i\theta_1 & \dots & 0 & 0 \\ \vdots & \vdots & \vdots & \vdots & \ddots & \vdots & \vdots \\ 0 & 0 & 0 & 0 & \dots & \cos i\theta_{d/2} & -\sin i\theta_{d/2-1} \\ 0 & 0 & 0 & 0 & \dots & \sin i\theta_{d/2} & \cos i\theta_{d/2-1} \end{bmatrix}$$

In Appendix A, we prove the availability of RoPE in the SSD algorithm. The algorithm matrix of the rotary position embedding is shown in Figure 2. In Appendix B.1, an implementation code example of RoPE and its application in Attn and SSD are provided.

3.2 Inner Function Attention with Dynamic Mask

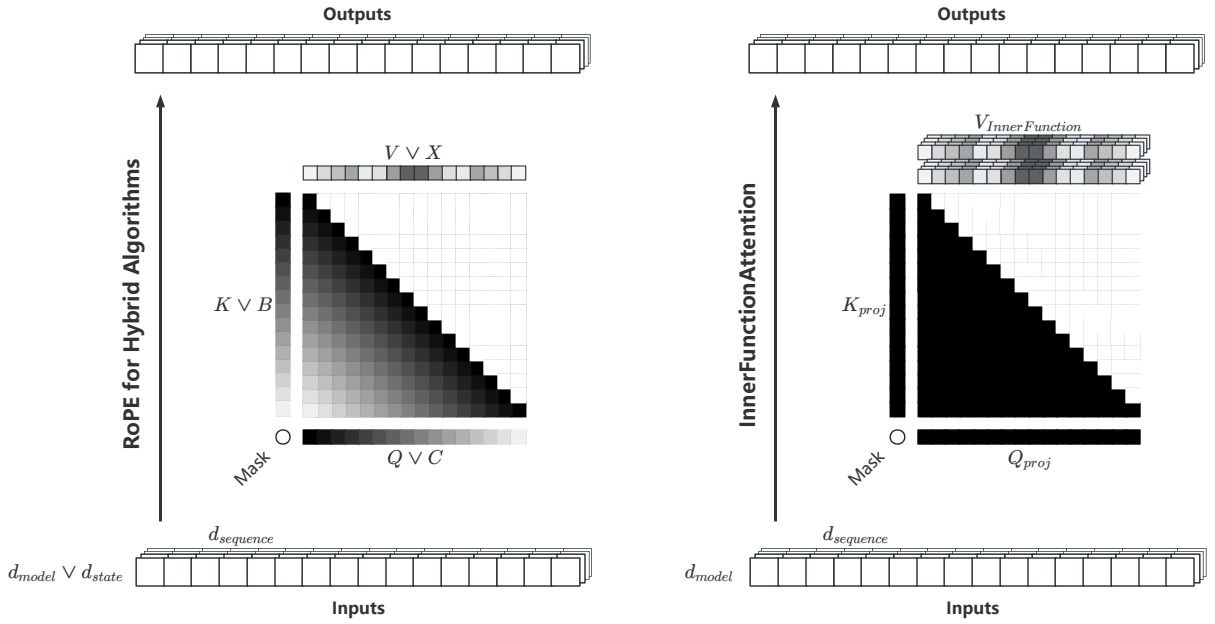


Figure 2: **(Left) RoPE for Hybrid Algorithms.** Shows the algorithm matrix of the rotary position embedding in the form of inner product. The depth of color represents the position of the position encoding, with higher color depth and lower color depth. The input tensor is first multiplied by the QK or CB matrix, then the sine and cosine position information is attached, and finally the relative position matrix of the scalar is obtained through the inner product operation. **(Right) Inner Function Attention.** Shows the structure and algorithm of inner function attention. The input tensor is first multiplied by QK to obtain the query and key matrix, then the scalar attention score is calculated, and finally the attention score is attached to the value state calculated by the inner function and output.

The QCAtn algorithm calculates the Q and K related to the entire input sequence x to form the attention matrix, and the hidden state (usually referred to as the KV cache) is a linearly growing list with t (token), explicitly storing all historical context information without any compression, and the time complexity of calculating this linearly growing state is quadratically increasing.

Inner Function. To enhance the expressive power of the hidden state of QCAtn, our idea is to transform part of the hidden state calculation from a simple $y = xW$ to an excellent heuristic $y = f(x)$. Considering that Q and K need to perform inner product operations, more complex operations may cause large fluctuations during training, so the heuristic

is applied to V . Of course, from a more intuitive perspective, queries and keys do only need simple linear transformations, and their dot product attention matrix determines which information to extract from the values. Therefore, we can apply the heuristic 3 to the value to improve the expressive power of the hidden state.

$$V_{innerfunc} = f(x) := (xW_{vQ}\theta_{vK}^T)W_V^T \times x \quad (3)$$

First, We initialize the parameters W_{vQ} , θ_{vK} , W_V . Where W_{vQ} and θ_{vK} are also very easy to expand into the multi-head, but for simplicity, we only show the basic computational framework. Where d_{model} represents the model hidden dimension, d_{ret} represents the retrieval dimension, n_v represents the number of values.

$$W_{vQ} \in \mathbb{R}^{d_{model} \times d_{ret}} \quad \theta_{vK} \in \mathbb{R}^{n_v \times d_{ret}} \quad W_V \in \mathbb{R}^{n_v \times d_{model}}$$

The second step is to perform matrix multiplication of the input state $x \in \mathbb{R}^{batch \times seq \times d_{model}}$ with W_{vQ} to obtain the low-rank projection of the input, and then perform dot product calculation with θ_{vK}^T to obtain the similarity scalar score g .

$$g = x \cdot W_{vQ} \cdot \theta_{vK}^T \in \mathbb{R}^{batch \times seq \times n_v}$$

The third step is to take the index of the topk values corresponding to the n_v dimension of g , obtaining i . It is worth noting that the output diversity increases with the increase of k .

$$i = \text{topk}(g, k, \text{dim} = -1).indices \in \mathbb{R}^{batch \times seq \times k}$$

The fourth step is to take out the values state of W_V^T corresponding to the index position i , obtaining v .

$$v = i \cdot W_V^T \in \mathbb{R}^{batch \times seq \times k \times d_{model}}$$

Finally, the values v are superimposed in the k dimension and associated with the input state x , obtaining V .

$$V = \sum_{i=1}^k x \times v_i \in \mathbb{R}^{batch \times seq \times d_{model}}$$

We assign the topk values with the highest affinity to each token, and all the weights of the values are shared rows, avoiding the problem of insufficient training caused by the sparse structure.

To retain the explicit storage of all historical context information by QCAttn, we still use the attention matrix calculated by QK^T to assign weight scores to the state $V_{innerfunc}$. However, the accuracy of the attention matrix score depends mainly on the dimension of n_{head} and the calculation accuracy of the *softmax* function. In very long contexts, a smaller n_{head} will cause the model lost in the middle (Liu et al. 2023), while a larger n_{head} will cause computational problems.

$$\begin{aligned} W_Q &\in \mathbb{R}^{d_{model} \times n_{heads} \times d_{head}} & W_K &\in \mathbb{R}^{d_{model} \times n_{heads} \times d_{head}} \\ Q &= xW_Q \in \mathbb{R}^{batch \times n_{heads} \times seq \times d_{head}} \\ K &= xW_K \in \mathbb{R}^{batch \times n_{heads} \times seq \times d_{head}} \\ A &= \text{softmax}(QK^T) \in \mathbb{R}^{batch \times n_{heads} \times seq \times seq} \end{aligned}$$

In general, we train transformers models using a tokenizer to pad the sequence to a fixed length for batch training. We use 0 to represent the attention mask of the padding part to ignore the information in this part when calculating the attention score. The attention mask of the original sequence part is usually all represented as 1, indicating that the information in this part is all valid. This static attention mask processing method is shown in the implementation example 5 in Appendix B.3.

Dynamic Attention Mask. The SSD algorithm uses $A \in \mathbb{R}^{n_{heads}}$ to selectively filter the previous state to prevent invalid information from affecting the current state. We imitate this selective mechanism and propose a simple plug-and-play dynamic mask method without changing the direction of community development. We move the function of creating the causal mask to the attention layer, add a learnable parameter 4, multiply it with the causal mask, the part originally filled with 0 will not change, and the effective part will be covered with noise as the dynamic mask parameter continues to learn, as shown in the implementation example 6 in Appendix B.3. This dynamic mask method is also stacked with the attention layer as the attention layer is stacked, thereby satisfying the selectivity of the sequence transformation state.

$$l := \text{round}(\text{ones}([n_{heads}, \text{max_position_len}])) \quad (4)$$

Finally, we apply the processed attention mask to the attention score matrix to ensure that the information extracted from the values is valid.

$$\begin{aligned} L &= \text{dynamic_mask}(l) \\ M &= L \circ A \\ y &= M \cdot V_{innerfunc} \end{aligned}$$

This inner function attention with dynamic attention mask can not only effectively expand the hidden state expressive power of sequence transformation but also reduce the error of scalar attention scores. The algorithm matrix of inner function attention is shown in Figure 2. An implementation code example of SSD is provided in Appendices B.2. An implementation code example of inner function attention is provided in Appendix B.3.

3.3 Cross Domain Mixture of Experts

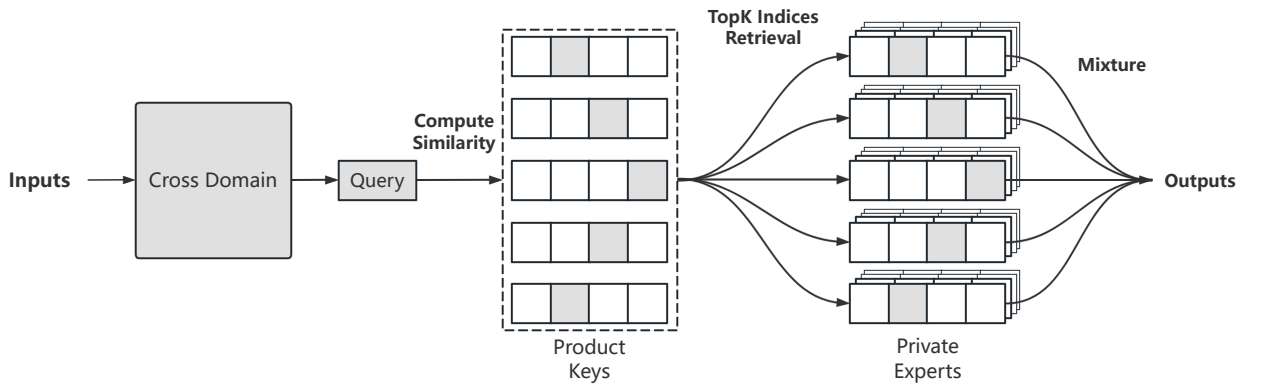


Figure 3: **CDMoE**. Shows the internal structure and calculation process of the cross domain million mixture of experts matrix. Input tensors first pass through the shared parameters of the cross domain, then pass through a linear layer and reshape into queries, then calculate the dot product with the keys to obtain the affinity with the private experts, and finally mix the tensors carrying shared knowledge through the top K private experts with the highest affinity.

In the conventional mixture of experts strategy, the tokens assigned to different experts need to have common knowledge or information, so multiple experts will have redundant parameters for storing common information when obtaining their

respective parameters, which leads to expert parameter redundancy. And the proportion of expert parameter redundancy increases with the increase in expert granularity and the decrease in the number of expert activations. In Mixture of A Million Experts (He 2024), due to the high granularity of the experts, even if all the expert weight rows are shared, the proportion of expert parameter redundancy reaches an astonishingly high level due to the low number of expert column activations, as can be seen from the loss curve starting from pre-training. So we propose a cross domain mixture of experts for two forms of equations 5, where e represents the expert, and N represents the number of experts.

$$e(x) = \sum_{i=1}^N e_i(x) + \phi(x) \quad e(x) = \sum_{i=1}^N e_i(\phi(x)) \quad (5)$$

Cross Domain. If the tokens assigned to different experts have already passed through the parameters for storing common knowledge, the parameter redundancy can be reduced. This parameter for storing common knowledge can be called cross domain. The output of the cross domain is used as the input of the private mixture of experts, and the mixture of experts will have an affinity calculation strategy to determine which expert to use, either a routing traversal strategy or a dot product score index strategy. This affinity calculation is equivalent to a gating mechanism used to determine which token should be processed by which expert, so we do not use a gated MLP as the cross domain. where s represents shared parameters, σ represents the activation function, W, V represents the two weight matrices of the MLP, d_{model} represents the model hidden dimension, and d_{ff} represents the representation dimension of the feedforward network.

$$\phi(x) = \sigma(xW^s)V^s \quad W^s \in \mathbb{R}^{d_{model} \times d_{ff}} \quad V^s \in \mathbb{R}^{d_{ff} \times d_{model}}$$

Efficient Retrieval Experts. Now we list an efficient retrieval expert $e(x)$ algorithm to complete the calculation of form equation two, because based on form two, you only need to adjust the calculation parameters to complete form equation one. First, we initialize the query projection matrix weight W_{eQ} , learnable key parameters θ_{eK} , and two weight matrices W_{edown} and W_{eup} . where p represents the private parameters, d_{ret} represents the expert retrieval state dimension, n_{expert} represents the number of experts, n_h represents the number of heads, and k represents the number of topk.

$$W_{eQ}^p \in \mathbb{R}^{d_{model} \times n_h \times d_{ret}} \quad \theta_{eK}^p \in \mathbb{R}^{n_h \times \sqrt{n_{expert}} \times d_{ret}} \quad W_{edown}^p \in \mathbb{R}^{n_{expert} \times d_{model}} \quad W_{eup}^p \in \mathbb{R}^{n_{expert} \times d_{model}}$$

The second step first performs matrix multiplication of the cross domain state information $\phi(x)$ with W_{eQ}^p to obtain the query projection of the shared knowledge, and then performs matrix multiplication with θ_{eK}^{pT} to obtain the dot product similarity g .

$$g = \phi(x) \cdot W_{eQ}^p \cdot \theta_{eK}^{pT} \in \mathbb{R}^{2 \times batch \times seq \times n_h \times \sqrt{n_{expert}}}$$

The third step takes the topk experts corresponding to each h in the $\sqrt{n_{expert}}$ dimension of g to obtain the scores and indices, and after some simple combination steps, obtains the scalar scores s and expert indices i .

$$s, i = \text{topk}(g, k, \text{dim} = -1) \in \mathbb{R}^{batch \times seq \times n_h \times k}$$

The fourth step performs matrix multiplication of the index position i with W_{edown}^{pT} and W_{eup}^{pT} , similar to embedding to expand the hidden dimension, taking out the weight rows of the expert dimension, obtaining the private state tensors d and u corresponding to the two index positions.

$$d, u = i \cdot W_{edown}^{pT}, i \cdot W_{eup}^{pT} \in \mathbb{R}^{batch \times seq \times n_h \times k \times d_{model}}$$

The fifth step performs matrix multiplication of the cross domain state $\phi(x)$ with d^T , then multiplies by the score s and non-linearly activates it to obtain the experts score $s(x)$.

$$s(x) = \sigma(\phi(x) \cdot d^T \times s) \in \mathbb{R}^{batch \times seq \times n_h \times k}$$

Finally, we first sum x and u in the n_h, k dimensions, then perform matrix multiplication of the expert score $s(x)$ with u , obtain the state of the private expert, and if you are worried that the non-linear activation in the previous step will destroy the cross domain state, then add it to $\phi(x)$ to obtain the final output y .

$$y = \sum_{i=1}^{n_h} \sum_{j=1}^k s(x)_{i,j} \cdot u_{i,j} + \phi(x) \in \mathbb{R}^{batch \times seq \times d_{model}}$$

This cross domain with efficient retrieval mixture of experts method not only has a large MLP to store the main state transformation information but also can dynamically combine different small MLPs in the n_h dimension. The small MLPs share neurons by aggregating the h singletons retrieved from the shared weight rows, which can efficiently retrieve the expert with the highest affinity for each token and maintain speed as the number of experts increases without rapid decline as in the routing strategy. The internal structure and calculation process of the cross domain mixture of experts matrix are shown in Figure 3. An implementation code example of CDMoE is provided in Appendix B.4.

3.4 Architecture Design

We designed an architecture using these matrices in the language modeling task: Cheems. In the model backbone, we use RoPE as the source of positional information before each sequence transformation module, and use a CDMoE module as the state transformation after the sequence transformation, with input normalization and residual connections between each sequence transformation and state transformation. In the sequence transformation combination method, we stack 7 SSD modules for each InnerFuncAttn module stacked (the stacking ratio comes from Transformers are SSMs (Dao and Gu 2024)), to ensure the model’s performance in multi-query contact recall tasks. The architecture of Cheems is shown in Figure 4.

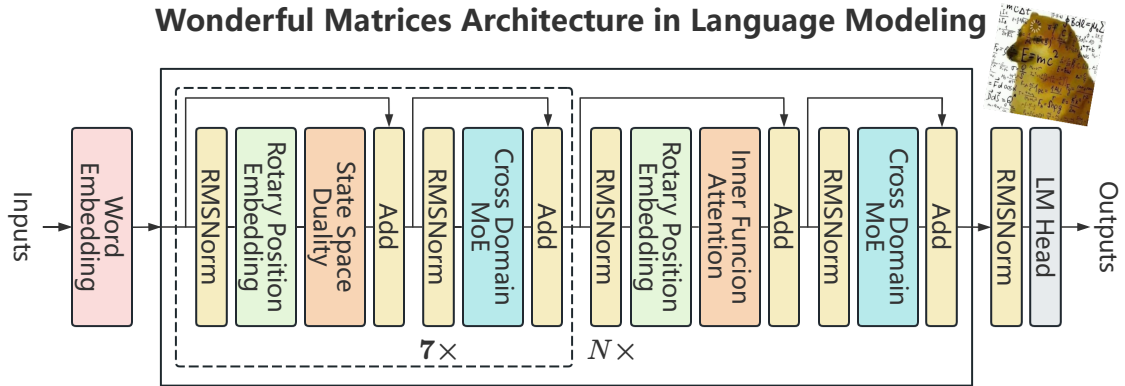


Figure 4: **Wonderful Matrices in Language Modeling: Cheems.** Shows the architecture of Wonderful Matrices applied in language modeling, including word embeddings, RMSNorm, Add (residual connection), RoPE, SSD, InnerFuncAttn, CDMoE, and LM Head modules. The black arrows indicate the calculation order of the modules, the black dashed lines indicate stacking this part 7 times, and the black solid lines indicate stacking the entire backbone module part N times. The dog in the upper right corner is the internet-famous Shiba Inu Cheems, which is our sense of humor, allowing us to relax and smile in strict formula derivation work. For the beauty of the partial table, in subsequent experiments, we will use Cheems as our model name.

4 Empirical Validation

4.1 Effect of Modules

Table 1: *Conv1d + D* vs. a_t vs. *RoPE*. In addition to the abbreviations mentioned above, we also use IFA to represent the InnerFuncAttn module and DM to represent the dynamic mask. In a single module, QCAtn cannot use *Conv1d + D* and a_t . With the sequence length set to 8192, the perplexity performance of all combined modules shows that *RoPE* is better than *Conv1d + D* and a_t .

MODULES	<i>Conv1d + D</i> PPL ↓	a_t PPL ↓	<i>RoPE</i> PPL ↓
QCAtn	—	—	8.38
SSD	8.56	8.62	8.33
SSD + QCAtn	8.48	8.56	8.18
SSD + IFA	8.43	8.49	8.12
SSD + IFA + DM	8.36	8.42	7.96

Table 2: **MLP vs. CDMoE**. We use S to represent the SSD module, A to represent the QCAtn module, M to represent the MLP module, and E to represent the CD-MoE module. We strictly construct different models with the same number of parameters, and the perplexity on the pre-training subset gradually decreases as the MoE ratio increases.

MODULES	MoE RATIO	PPL ↓
SMSMSMSMSMSMSMA	0%	8.18
SE SMSMSMSMSMSMA	6.25%	8.06
SMSMSMSMSMSMSMAE	6.25%	8.12
SE SMSMSMSMSMSMAE	12.5%	7.96
SM SE SE SE SE SE SE AE	37.5%	7.52
SE SE SE SE SE SE SE AE	50%	7.49

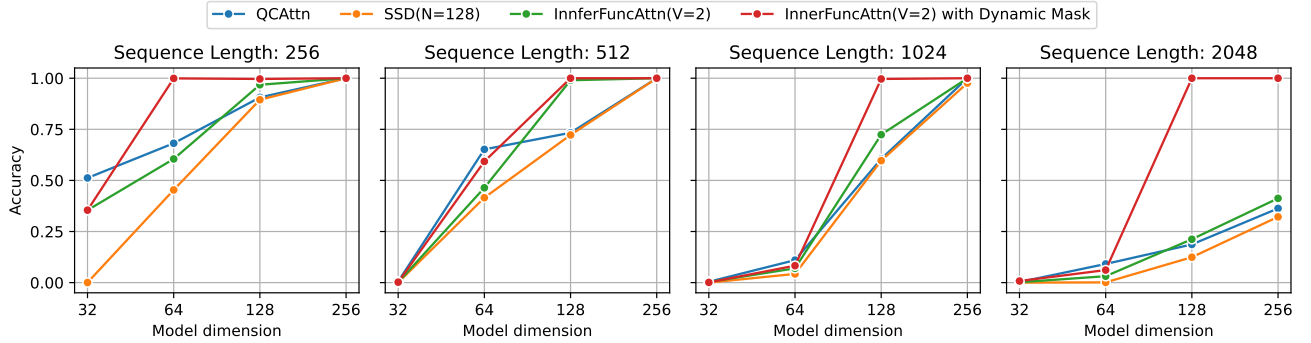


Figure 5: **Multi-Query Associative Recall**. We introduced a more difficult version of the original multi-query associative recall task (Arora et al. 2024), including longer sequence lengths, smaller model dimensions, etc. For detailed parameters, see Appendix C.1. InnerFuncAttn with Dynamic Mask maintains good performance in most cases.

In Table 1, we can see that whether using the SSD algorithm alone, the QCAtn algorithm, or a combination of the two, RoPE has the best perplexity performance on long sequences. This is also the case when using InnerFuncAttn and dynamic masks.

In Table 2, we can see that as the proportion of CDMoE in the entire model increases, the perplexity of the model on the pre-training subset gradually decreases. However, we also found that using a fully dense activation MLP module in the first and last state transformations is not much different from using all CDMoE, which may increase the stability of the model output. However, for the sake of simple modeling, we chose to use all CDMoE.

In Table 3, we can see that CDMoE achieved the best results on all tasks in CEvalBenchmark. The model parameters are similar to the 1.3B scale parameter settings in Table 7. At the same time, we also have to admire the high quality of the Smollm-Corpus (Ben Allal et al. 2024) and Chinese Cosmopedia datasets. Compared with using other training datasets, mixing training with them increased the accuracy of these three models by about 10%, especially in the five-shot.

In Figure 5, we show the performance of QCAtn, SSD, InnerFuncAttn, and InnerFuncAttn with Dynamic Mask in the multi-query associative recall task. We can see that when the model dimension reaches 128, and InnerFuncAttn allocates 64 dimensions for each V , InnerFuncAttn is more accurate than QCAtn and SSD. When the sequence length is extended to 2048, the contact recall capabilities of the three structures are limited by sequence noise, but InnerFuncAttn with Dynamic Mask still maintains good performance.

Table 3: **MoE vs. MoE-SEI vs. CDMoE in CEvalBenchmark**. These tasks come from CEvalBenchmark (Huang et al. 2023), we keep the sequence transformation part of the Cheems architecture unchanged, and use three sparse activation mixture of experts as state transformation to construct three models with almost the same total parameters and activation parameters. We detail the zero-shot and five-shot accuracy of these three architectures on each subtask. CDMoE achieved the best results on all tasks.

Task	MoE	MoE-SEI	CDMoE	MoE	MoE-SEI	CDMoE
	ZERO-SHOT \uparrow	ZERO-SHOT \uparrow	ZERO-SHOT \uparrow	FIVE-SHOT \uparrow	FIVE-SHOT \uparrow	FIVE-SHOT \uparrow
computer network	50.11	58.74	61.07	52.95	60.23	62.36
operating system	57.83	63.88	65.52	57.83	54.64	55.28
computer architecture	60.17	58.94	61.25	60.17	56.64	61.5
college programming	37.34	38.9	42.42	37.48	38.9	41.81
college physics	44.2	40.12	45.98	43.7	45.98	45.98
college chemistry	27.17	50.74	65.03	52.73	70.15	71.5
advanced mathematics	42.9	44.45	48.52	45.15	48.52	48.88
probability and statistics	51.82	51.82	47.8	43.32	46.77	50.9
discrete mathematics	38.8	45.55	41.58	38.8	40.56	42.46
electrical engineer	43.86	48.17	51.53	48.17	58.12	61.99
metrology engineer	41.39	40.11	44.04	42.02	44.0	49.87
high school mathematics	44.07	46.4	47.8	44.91	46.4	48.05
high school physics	59.05	63.65	64.17	54.0	57.3	63.42
high school chemistry	24.06	55.32	57.6	24.49	55.32	57.87
high school biology	52.24	52.24	51.83	53.76	60.57	61.41
middle school mathematics	65.93	69.27	69.65	65.38	69.27	69.99
middle school biology	40.65	40.95	40.65	40.65	40.95	41.68
middle school physics	62.47	62.47	63.5	49.38	50.88	57.16
middle school chemistry	44.58	46.31	53.66	44.58	44.58	52.14
veterinary medicine	48.86	53.92	55.11	48.86	54.63	55.89
college economics	26.34	39.64	36.89	29.06	35.5	39.64
business administration	39.88	38.68	38.68	41.67	46.28	49.14
marxism	52.59	58.68	61.2	55.88	61.65	63.23
mao zedong thought	10.91	27.62	35.47	13.39	26.99	35.47
education science	34.38	36.18	35.41	34.75	37.14	37.14
teacher qualification	32.69	34.19	32.69	34.08	37.37	39.15
high school politics	71.84	71.13	74.56	71.84	74.94	78.4
high school geography	55.46	55.46	55.46	55.11	55.46	56.0
middle school politics	35.18	38.81	39.75	32.83	38.51	41.44
middle school geography	75.96	78.92	76.47	49.23	50.81	66.8
modern chinese history	50.31	49.34	58.36	64.35	66.02	68.61
ideological and moral cultivation	27.76	51.07	53.53	30.46	47.32	51.07
logic	61.48	61.48	61.48	59.58	61.48	60.47
law	49.45	54.14	55.25	52.27	59.31	60.38
chinese language and literature	57.36	60.78	62.24	57.04	60.78	64.17
art studies	33.44	32.5	32.27	33.44	35.86	34.1
professional tour guide	50.89	52.36	52.63	48.07	48.07	51.18
legal professional	48.6	55.29	55.29	50.25	58.63	58.13
high school chinese	50.6	50.6	55.08	51.15	54.02	65.06
high school history	33.77	47.0	47.0	43.08	57.45	59.07
middle school history	52.11	50.37	52.11	44.26	46.16	52.11
civil servant	32.97	32.65	34.83	34.34	36.9	35.07
sports science	38.16	50.13	61.8	63.21	77.19	69.0
plant protection	45.81	50.45	49.17	44.73	50.45	48.47
basic medicine	61.37	67.15	67.15	56.81	62.71	64.27
clinical medicine	44.37	54.22	56.99	39.3	44.37	49.6
urban and rural planner	39.01	42.95	40.43	39.54	42.95	41.06
accountant	22.8	34.15	38.45	24.56	36.15	38.45
fire engineer	33.15	32.2	37.44	35.51	40.09	41.2
environmental impact assessment	39.7	50.42	50.42	39.26	50.42	50.42
tax accountant	27.1	36.27	44.03	26.3	34.14	39.75
physician	30.34	36.27	36.98	33.74	39.82	41.4
Average	44.29	49.29	51.31	44.95	50.37	52.88

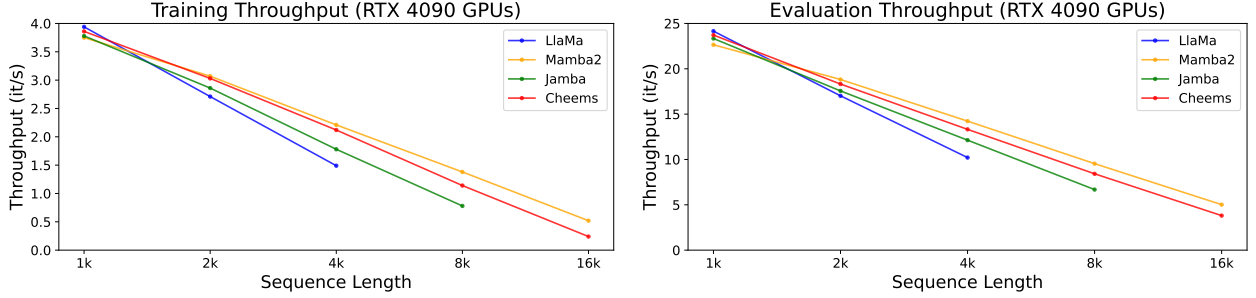


Figure 6: **Efficient Benchmark.** The LLaMa architecture that uses QCAtn as the sequence transformation, the Mamba2 architecture that uses SSD as the sequence transformation, the Jamba architecture that uses SSD and QCAtn as the sequence transformation, and the Cheems architecture proposed in this paper. These architectures are train (both forward and backward) and valid (forward only) at different sequence lengths under the 1.3B parameter scale. Cheems is more efficient than LLaMa and Jamba, but slightly lower than Mamba2.

Table 4: **Effective Benchmark.** The LLaMa architecture that uses QCAtn as the sequence transformation and MoE-SEI as the state transformation, the Mamba2 architecture that uses SSD as the sequence transformation and MoE-SEI as the state transformation, the Jamba architecture that uses SSD and QCAtn as the sequence transformation and MoE-SEI as the state transformation, and the Cheems architecture proposed in this paper. The verification results of the models trained under the same conditions. The best results for each parameter scale are shown in bold, followed by underline. For each model parameter scale, Cheems performs better than other models in most cases. We do not provide the perplexity performance of pre-training because the model training completion time is before the gradient accumulation error fix in the transformers library, and there is no reference value for using different gradient accumulation steps before the fix and new experiments after the fix. If our training results are reproduced in the future, the scores on these verification metrics may rise. For the introduction of the verification set and the specific model parameters, see Appendix C.2.

MODEL	MMLU ACC ↑	TRIVIAQA QEM ↑	ARC ACC ↑	PIQA ACC ↑	HELLASWAG ACC ↑	OBQA ACC ↑	WINOGRANDE ACC ↑	AVG
LlaMa-320M	<u>33.65</u>	8.86	51.68	71.42	52.30	<u>37.02</u>	53.15	43.99
Mamba2-320M	33.10	<u>9.36</u>	50.72	70.24	48.62	35.16	54.17	43.07
Jamba-320M	33.12	9.32	50.80	<u>71.88</u>	<u>52.92</u>	36.73	<u>55.24</u>	<u>44.31</u>
Cheems-320M	34.45	10.38	<u>51.57</u>	73.32	53.79	37.42	55.61	45.22
LlaMa-1.3B	<u>37.86</u>	20.66	59.82	76.05	61.65	41.15	55.40	50.36
Mamba2-1.3B	36.28	21.28	58.02	72.26	59.48	37.98	58.72	49.07
Jamba-1.3B	37.43	<u>21.60</u>	59.33	<u>76.58</u>	<u>62.33</u>	40.82	<u>59.20</u>	<u>51.07</u>
Cheems-1.3B	39.08	23.02	<u>59.69</u>	78.15	63.63	<u>41.12</u>	62.09	52.44

4.2 Language Modeling

We selected LLaMa (Touvron et al. 2023), Mamba2 (Dao and Gu 2024), and Jamba (Lieber et al. 2024) as the comparison objects for Cheems. In Figure 6, we can see that the forward and backward propagation efficiency of Cheems has surpassed LLaMa and Jamba, and maintains a lower gap with Mamba2. In Table 4, we can see that Cheems performs better than LLaMa, Mamba2, and Jamba on most verification metrics. And as the parameter scale increases, the performance improvement of Cheems is more significant.

5 Discussion

In fact, we encountered many problems when completing this work, including various reasons that caused the mamba-ssm library to not work properly. Before solving this problem, we tried to directly remove the SSD sequence transformation module and modify the architecture to stack multiple MLP or MoE state transformation modules after a single Attn

sequence transformation module, as shown in Figure 7. We found that using this model architecture, ensuring that the number of parameters is equal to or less than the Transformer architecture for language modeling, there is no significant decrease in most verification metrics. We speculate that in the current Transformer architecture, the Attn layer may have some redundancy. Research on the impact of model layer attention scores on depth and reducing attention redundancy may be a future research direction.

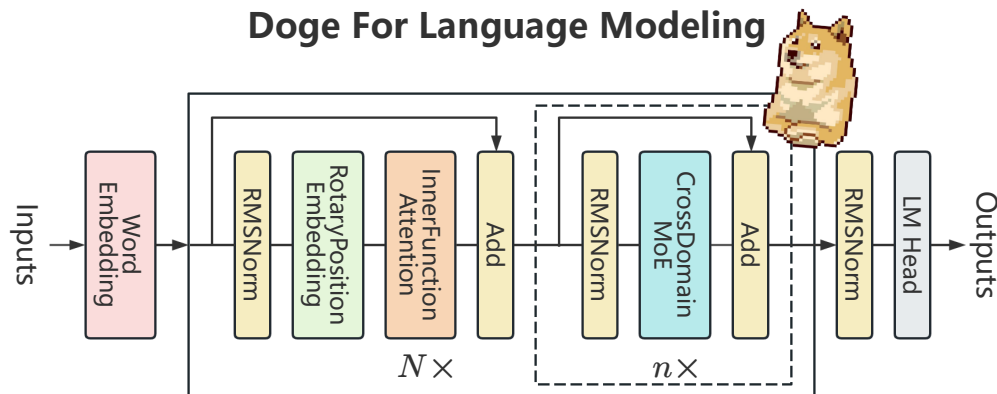


Figure 7: **Doge Architecture**. Remove the SSD sequence transformation module in the Cheems architecture and modify the architecture to stack multiple CDMoE state transformation modules after a single InnerFuncAttn sequence transformation module.

6 Conclusion

This paper explores the idea of modeling by integrating the state space duality algorithm with the quadratic causal self-attention algorithm. We studied the efficient positional encoding under the fusion algorithm, the internal function attention with dynamic mask that can enhance the expressive power, and the cross domain mixture of experts that reduces parameter redundancy. Finally, we verified that these algorithms have reached the advanced level in language modeling performance, promoting the development of language modeling in a more efficient and effective direction.

Acknowledgments

We thank our families for their understanding and support in completing this work as independent researchers. At the same time, we also thank Professor Albert Gu of Carnegie Mellon University for providing us with an endorsement of ArXiv, allowing us to engage in scientific research at the undergraduate level.

References

- [1] Joshua Ainslie, James Lee-Thorp, Michiel de Jong, Yury Zemlyanskiy, Federico Lebrón, and Sumit Sanghai. “GQA: Training Generalized Multi-Query Transformer Models from Multi-Head Checkpoints”. In: *arXiv preprint arXiv:2305.13245* (2023).
- [2] Simran Arora, Sabri Eyuboglu, Aman Timalsina, Isys Johnson, Michael Poli, James Zou, Atri Rudra, and Christopher Ré. “Zoology: Measuring and Improving Recall in Efficient Language Models”. In: *The International Conference on Learning Representations (ICLR)*. 2024.
- [3] Loubna Ben Allal, Anton Lozhkov, Guilherme Penedo, Thomas Wolf, and Leandro von Werra. *SmolLM-Corpus*. 2024. URL: <https://huggingface.co/datasets/HuggingFaceTB/smolLM-corpus>.
- [4] Yonatan Bisk, Rowan Zellers, Jianfeng Gao, Yejin Choi, et al. “PIQA: Reasoning about Physical Commonsense in Natural Language”. In: *Proceedings of the AAAI conference on Artificial Intelligence*. Vol. 34. 2020.
- [5] Peter Clark, Isaac Cowhey, Oren Etzioni, Tushar Khot, Ashish Sabharwal, Carissa Schoenick, and Oyvind Tafjord. “Think you have Solved Question Answering? Try ARC, the AI2 Reasoning Challenge”. In: *arXiv preprint arXiv:1803.05457* (2018).

- [6] Damai Dai, Chengqi Deng, Chenggang Zhao, R. X. Xu, Huazuo Gao, Deli Chen, Jiashi Li, Wangding Zeng, Xingkai Yu, Y. Wu, Zhenda Xie, Y. K. Li, Panpan Huang, Fuli Luo, Chong Ruan, Zhifang Sui, and Wenfeng Liang. “DeepSeek-MoE: Towards Ultimate Expert Specialization in Mixture-of-Experts Language Models”. In: *CoRR* abs/2401.06066 (2024). URL: <https://arxiv.org/abs/2401.06066>.
- [7] Tri Dao and Albert Gu. “Transformers are SSMs: Generalized Models and Efficient Algorithms Through Structured State Space Duality”. In: *International Conference on Machine Learning (ICML)*. 2024.
- [8] Leo Gao, Jonathan Tow, Stella Biderman, Sid Black, Anthony DiPofi, Charles Foster, Laurence Golding, Jeffrey Hsu, Kyle McDonell, Niklas Muennighoff, Jason Phang, Laria Reynolds, Eric Tang, Anish Thite, Ben Wang, Kevin Wang, and Andy Zou. *A Framework for Few-shot Language Model Evaluation*. Version v0.0.1. Sept. 2021. DOI: [10.5281/zenodo.5371628](https://doi.org/10.5281/zenodo.5371628). URL: <https://doi.org/10.5281/zenodo.5371628>.
- [9] Albert Gu and Tri Dao. “Mamba: Linear-Time Sequence Modeling with Selective State Spaces”. In: *arXiv preprint arXiv:2312.00752* (2023).
- [10] Xu Owen He. “Mixture of A Million Experts”. In: *arXiv preprint arXiv:2407.04153* (2024).
- [11] Dan Hendrycks, Collin Burns, Steven Basart, Andy Zou, Mantas Mazeika, Dawn Song, and Jacob Steinhardt. *Measuring Massive Multitask Language Understanding*. 2021. arXiv: [2009.03300](https://arxiv.org/abs/2009.03300) [cs.CY]. URL: <https://arxiv.org/abs/2009.03300>.
- [12] Yuzhen Huang, Yuzhuo Bai, Zhihao Zhu, Junlei Zhang, Jinghan Zhang, Tangjun Su, Junteng Liu, Chuancheng Lv, Yikai Zhang, Jiayi Lei, Yao Fu, Maosong Sun, and Junxian He. “C-Eval: A Multi-Level Multi-Discipline Chinese Evaluation Suite for Foundation Models”. In: *Advances in Neural Information Processing Systems*. 2023.
- [13] Mandar Joshi, Eunsol Choi, Daniel S. Weld, and Luke Zettlemoyer. *TriviaQA: A Large Scale Distantly Supervised Challenge Dataset for Reading Comprehension*. 2017. arXiv: [1705.03551](https://arxiv.org/abs/1705.03551) [cs.CL].
- [14] Angelos Katharopoulos, Apoorv Vyas, Nikolaos Pappas, and François Fleuret. “Transformers are RNNs: Fast Autoregressive Transformers with Linear Attention”. In: *International Conference on Machine Learning*. PMLR. 2020, pp. 5156–5165.
- [15] Opher Lieber, Barak Lenz, Hofit Bata, Gal Cohen, Jhonathan Osin, Itay Dalmedigos, Erez Safahi, Shaked Meirom, Yonatan Belinkov, Shai Shalev-Shwartz, et al. “Jamba: A Hybrid Transformer-Mamba Language Model”. In: *arXiv preprint arXiv:2403.19887* (2024).
- [16] Nelson F. Liu, Kevin Lin, John Hewitt, Ashwin Paranajpe, Michele Bevilacqua, Fabio Petroni, and Percy Liang. *Lost in the Middle: How Language Models Use Long Contexts*. 2023. arXiv: [2307.03172](https://arxiv.org/abs/2307.03172) [cs.CL]. URL: <https://arxiv.org/abs/2307.03172>.
- [17] Todor Mihaylov, Peter Clark, Tushar Khot, and Ashish Sabharwal. “Can a Suit of Armor Conduct Electricity? A New Dataset for Open Book Question Answering”. In: *arXiv preprint arXiv:1809.02789* (2018).
- [18] Meta NVIDIA. *PyTorch Container Image*. <https://catalog.ngc.nvidia.com/orgs/nvidia/containers/pytorch>. 2022.
- [19] Keisuke Sakaguchi, Ronan Le Bras, Chandra Bhagavatula, and Yejin Choi. “Winogrande: An Adversarial Winograd Schema Challenge at Scale”. In: *Communications of the ACM* 64.9 (2021), pp. 99–106.
- [20] Jianlin Su, Yu Lu, Shengfeng Pan, Ahmed Murtadha, Bo Wen, and Yunfeng Liu. “Roformer: Enhanced Transformer with Rotary Position Embedding”. In: *arXiv preprint arXiv:2104.09864* (2021).
- [21] Yu Sun, Xinhao Li, Karan Dalal, Jiarui Xu, Arjun Vikram, Genghan Zhang, Yann Dubois, Xinlei Chen, Xiaolong Wang, Sanmi Koyejo, Tatsunori Hashimoto, and Carlos Guestrin. “Learning to (Learn at Test Time): RNNs with Expressive Hidden States”. In: *arXiv preprint arXiv:2407.04620* (2024).
- [22] Hugo Touvron, Louis Martin, Kevin Stone, Peter Albert, Amjad Almahairi, Yasmine Babaei, Nikolay Bashlykov, Soumya Batra, Prajjwal Bhargava, Shruti Bhosale, et al. “Llama 2: Open foundation and fine-tuned chat models”. In: *arXiv preprint arXiv:2307.09288* (2023).
- [23] Ashish Vaswani, Noam Shazeer, Niki Parmar, Jakob Uszkoreit, Llion Jones, Aidan N. Gomez, Lukasz Kaiser, and Illia Polosukhin. “Attention Is All You Need”. In: *Advances in Neural Information Processing Systems (NeurIPS)*. 2017.
- [24] Thomas Wolf, Lysandre Debut, Victor Sanh, Julien Chaumond, Clement Delangue, Anthony Moi, Pierric Cistac, Tim Rault, Rémi Louf, Morgan Funtowicz, Joe Davison, Sam Shleifer, Patrick von Platen, Clara Ma, Yacine Jernite, Julien Plu, Canwen Xu, Teven Le Scao, Sylvain Gugger, Mariama Drame, Quentin Lhoest, and Alexander M. Rush. “Transformers: State-of-the-Art Natural Language Processing”. In: *Proceedings of the 2020 Conference on Empirical Methods in Natural Language Processing: System Demonstrations*. Online: Association for Computational Linguistics, Oct. 2020, pp. 38–45. URL: <https://www.aclweb.org/anthology/2020.emnlp-demos.6>.
- [25] Rowan Zellers, Ari Holtzman, Yonatan Bisk, Ali Farhadi, and Yejin Choi. “HellaSwag: Can a Machine Really Finish Your Sentence?” In: *Proceedings of the 57th Annual Meeting of the Association for Computational Linguistics*. 2019.

A RoPE for SSD

Proof of equation 2. by definition, $h_0 = B_0x_0$. By induction,

$$\begin{aligned} h_t &= A_t \dots A_1 B_0 x_0 + A_t \dots A_2 B_1 x_1 + \dots + A_t A_{t-1} B_{t-2} x_{t-2} + A_t B_{t-1} x_{t-1} + B_t x_t \\ &= \sum_{s=0}^t A_{t:s}^\times B_s x_s \end{aligned}$$

Multiplying by C_t to produce y_t , and vectorizing the equation to $t \in [T]$ (T is the sequence length), we derive the matrix transformation form of SSD.

$$\begin{aligned} y_t &= \sum_{s=0}^t C_t^\top A_{t:s}^\times B_s x_s \\ y &= \text{SSD}(A, B, C)(x) = Mx \\ M_{ji} &:= C_j^\top A_j \dots A_{i+1} B_i \end{aligned}$$

Then the matrix form of SSD is represented using SSS (Sequentially Semiseparable) as $M = \text{SSS}(A, B, C)$, where $M_{ji} = C_j^\top A_{j:i} B_i$, and then considering A is just a scalar, rearranged as

$$M_{ji} = A_{j:i} \cdot (C_j^\top B_i)$$

Vectorized as

$$\begin{aligned} L &:= \text{1SS}(a) \\ M &= L \circ (CB^\top) \end{aligned}$$

Finally, it is proved that the matrix transformation form of SSD is equivalent to Attention $(L \circ QK^\top) \cdot V = (L \circ CB^\top) \cdot X$.

Now we have enough theoretical support to give rotational positional encoding to the C and B matrices in SSD.

$$\begin{aligned} C_j &= f_C(x_j, j) \\ B_i &= f_B(x_i, i) \end{aligned}$$

C_j represents the output weight matrix of the j -th token corresponding to the word vector x_j integrated with the position information j , B_i represents the input weight matrix of the i -th token corresponding to the word vector x_i integrated with the position information i .

To utilize the relative positional information between tokens, we assume that the inner product operation between the C_j vector and the B_i vector can be represented by a function g , where the input of the function g is the word embedding vectors x_j and x_i , and their relative positional information $j - i$, the inner product of C_j and B_i and their relative positional information $j - i$ is defined as

$$\langle f_C(x_j, j), f_B(x_i, i) \rangle = g(x_j, x_i, j - i)$$

Now, assuming the word embedding vector dimension is $d = 2$, we have $f_C(x_j, j) = (W_C x_j) e^{ij\theta}$, for the first half of the formula $W_C x_j$, we know that W_C is a two-dimensional matrix, x_j is a two-dimensional vector, the result of the multiplication is naturally a two-dimensional vector, represented by C_j

$$C_j = \begin{bmatrix} C_j^{(1)} \\ C_j^{(2)} \end{bmatrix} = W_C x_j = \begin{bmatrix} W_C^{(11)} & W_C^{(12)} \\ W_C^{(21)} & W_C^{(22)} \end{bmatrix} \begin{bmatrix} x_j^{(1)} \\ x_j^{(2)} \end{bmatrix}$$

For the second half $e^{ij\theta}$, according to Euler's formula $e^{ix} = \cos(x) + \iota \sin(x)$, we have

$$e^{ij\theta} = \cos(j\theta) + \iota \sin(j\theta)$$

We know

$$f_C(x_j, j) = (W_C x_j) e^{ij\theta} = C_j e^{ij\theta}$$

C_j is represented in complex form,

$$C_j = [C_j^{(1)}, C_j^{(2)}] = [C_j^{(1)} + \iota C_j^{(2)}]$$

Thus,

$$f_C(x_j, j) = C_j e^{ij\theta} = [C_j^{(1)} + \iota C_j^{(2)}] e^{ij\theta}$$

According to the above derivation, we know that $f_C(x_j, j)$ is the product of two complex numbers,

$$f_C(x_j, j) = C_j e^{ij\theta} = [C_j^{(1)} + \iota C_j^{(2)}] \times (\cos(j\theta) + \iota \sin(j\theta))$$

Considering the following two formulas about complex numbers

$$(a + \iota b) \times (c + \iota d) = ac + \iota bc + \iota ad + \iota^2 bd = (ac - bd) + \iota(bc + ad)$$

$$\iota^2 = -1$$

We have

$$C_j e^{ij\theta} = [C_j^{(1)} + \iota C_j^{(2)}] \times (\cos(j\theta) + \iota \sin(j\theta)) = [C_j^{(1)} \cos(j\theta) - C_j^{(2)} \sin(j\theta)] + \iota [C_j^{(2)} \cos(j\theta) + C_j^{(1)} \sin(j\theta)]$$

Expressing this result as a real vector,

$$C_j e^{ij\theta} = [C_j^{(1)} \cos(j\theta) - C_j^{(2)} \sin(j\theta), C_j^{(2)} \cos(j\theta) + C_j^{(1)} \sin(j\theta)]$$

Therefore, C_j multiplied by a rotation matrix is obtained.

$$\begin{aligned} f_C(x_j, j) &= (W_C x_j) e^{ij\theta} = C_j e^{ij\theta} \\ &= \begin{bmatrix} C_j^{(1)} \cos(j\theta) - C_j^{(2)} \sin(j\theta), C_j^{(2)} \cos(j\theta) + C_j^{(1)} \sin(j\theta) \end{bmatrix} \\ &= \begin{bmatrix} \cos(j\theta) & -\sin(j\theta) \\ \sin(j\theta) & \cos(j\theta) \end{bmatrix} \begin{bmatrix} C_j^{(1)} \\ C_j^{(2)} \end{bmatrix} \end{aligned}$$

Similarly, B_i vector can be obtained

$$\begin{aligned} f_B(x_i, i) &= (W_B x_i) e^{ii\theta} = B_i e^{ii\theta} \\ &= \begin{bmatrix} B_i^{(1)} \cos(i\theta) - B_i^{(2)} \sin(i\theta), B_i^{(2)} \cos(i\theta) + B_i^{(1)} \sin(i\theta) \end{bmatrix} \\ &= \begin{bmatrix} \cos(i\theta) & -\sin(i\theta) \\ \sin(i\theta) & \cos(i\theta) \end{bmatrix} \begin{bmatrix} B_i^{(1)} \\ B_i^{(2)} \end{bmatrix} \end{aligned}$$

The function g can be represented as

$$g(x_j, x_i, j - i) = \Re \left[(W_C x_j) (W_B x_i)^* e^{i(j-i)\theta} \right]$$

where \Re represents the real part of the complex number x , $(W_C x_j) (W_B x_i)^*$ represents the conjugate of the product of two complex numbers. Considering

$$\begin{aligned} z &= a + ib \\ z^* &= a - ib \end{aligned}$$

we have

$$\begin{aligned} W_C x_j &= C_j = C_j^{(1)} + iC_j^{(2)} \\ W_B x_i &= B_i = B_i^{(1)} + iB_i^{(2)} \\ (W_B x_i)^* &= B_i^* = B_i^{(1)} - iB_i^{(2)} \\ e^{i(j-i)\theta} &= \cos((j-i)\theta) + i\sin((j-i)\theta) \end{aligned}$$

We now want to prove that

$$\begin{aligned} g(x_j, x_i, j - i) &= \Re \left[(W_C x_j) (W_B x_i)^* e^{i(j-i)\theta} \right] \\ &= \Re \left[(C_j^{(1)} + iC_j^{(2)}) (B_i^{(1)} - iB_i^{(2)}) (\cos((j-i)\theta) + i\sin((j-i)\theta)) \right] \\ &= \Re \left[((C_j^{(1)} B_i^{(1)} + C_j^{(2)} B_i^{(2)}) + i(C_j^{(2)} B_i^{(1)} - C_j^{(1)} B_i^{(2)})) (\cos((j-i)\theta) + i\sin((j-i)\theta)) \right] \\ &= (C_j^{(1)} B_i^{(1)} + C_j^{(2)} B_i^{(2)}) \cos((j-i)\theta) - (C_j^{(2)} B_i^{(1)} - C_j^{(1)} B_i^{(2)}) \sin((j-i)\theta) \end{aligned}$$

Recalling the vectorized form of SSD, the C vector at position j and the B vector at position i will perform an inner product operation, that is,

$$\begin{aligned} f_C(x_j, j) &= \left[C_j^{(1)} \cos(j\theta) - C_j^{(2)} \sin(j\theta), C_j^{(2)} \cos(j\theta) + C_j^{(1)} \sin(j\theta) \right] \\ f_B(x_i, i) &= \left[B_i^{(1)} \cos(i\theta) - B_i^{(2)} \sin(i\theta), B_i^{(2)} \cos(i\theta) + B_i^{(1)} \sin(i\theta) \right] \end{aligned}$$

We have

$$\begin{aligned} \langle f_C(x_j, j), f_B(x_i, i) \rangle &= \left[C_j^{(1)} \cos(j\theta) - C_j^{(2)} \sin(j\theta) \right] \left[B_i^{(1)} \cos(i\theta) - B_i^{(2)} \sin(i\theta) \right] \\ &\quad + \left[C_j^{(2)} \cos(j\theta) + C_j^{(1)} \sin(j\theta) \right] \left[B_i^{(2)} \cos(i\theta) + B_i^{(1)} \sin(i\theta) \right] \\ &= C_j^{(1)} \cos(j\theta) B_i^{(1)} \cos(i\theta) - C_j^{(1)} \cos(j\theta) B_i^{(2)} \sin(i\theta) \\ &\quad - C_j^{(2)} \sin(j\theta) B_i^{(1)} \cos(i\theta) + C_j^{(2)} \sin(j\theta) B_i^{(2)} \sin(i\theta) \\ &\quad + C_j^{(2)} \cos(j\theta) B_i^{(2)} \cos(i\theta) + C_j^{(2)} \cos(j\theta) B_i^{(1)} \sin(i\theta) \\ &\quad + C_j^{(1)} \sin(j\theta) B_i^{(2)} \cos(i\theta) + C_j^{(1)} \sin(j\theta) B_i^{(1)} \sin(i\theta) \end{aligned}$$

Considering

$$\begin{aligned} \sin(a + b) &= \sin(a) \cos(b) + \cos(a) \sin(b) \\ \sin(a - b) &= \sin(a) \cos(b) - \cos(a) \sin(b) \\ \cos(a + b) &= \cos(a) \cos(b) - \sin(a) \sin(b) \\ \cos(a - b) &= \cos(a) \cos(b) + \sin(a) \sin(b) \end{aligned}$$

We have

$$\begin{aligned} \langle f_C(x_j, j), f_B(x_i, i) \rangle &= C_j^{(1)} B_i^{(1)} (\cos(j\theta) \cos(i\theta) + \sin(j\theta) \sin(i\theta)) \\ &\quad + C_j^{(1)} B_i^{(2)} (-\cos(j\theta) \sin(i\theta) + \sin(j\theta) \cos(i\theta)) \\ &\quad + C_j^{(2)} B_i^{(1)} (-\sin(j\theta) \cos(i\theta) + \cos(j\theta) \sin(i\theta)) \\ &\quad + C_j^{(2)} B_i^{(2)} (\sin(j\theta) \sin(i\theta) + \cos(j\theta) \cos(i\theta)) \\ &= C_j^{(1)} B_i^{(1)} \cos((j - i)\theta) + C_j^{(1)} B_i^{(2)} \sin((j - i)\theta) \\ &\quad - C_j^{(2)} B_i^{(1)} \sin((j - i)\theta) + C_j^{(2)} B_i^{(2)} \cos((j - i)\theta) \\ &= (C_j^{(1)} B_i^{(1)} + C_j^{(2)} B_i^{(2)}) \cos((j - i)\theta) + (C_j^{(1)} B_i^{(2)} - C_j^{(2)} B_i^{(1)}) \sin((j - i)\theta) \\ &= (C_j^{(1)} B_i^{(1)} + C_j^{(2)} B_i^{(2)}) \cos((j - i)\theta) - (C_j^{(2)} B_i^{(1)} - C_j^{(1)} B_i^{(2)}) \sin((j - i)\theta) \\ &= g(x_j, x_i, j - i) \end{aligned}$$

It is proved that the inner product of the C vector at position j and the B vector at position i is the function g .

Finally, using the matrix-vector multiplication form

$$\begin{aligned}
\langle f_C(x_j, j), f_B(x_i, i) \rangle &= \left[\begin{bmatrix} \cos(j\theta) & -\sin(j\theta) \\ \sin(j\theta) & \cos(j\theta) \end{bmatrix} \begin{bmatrix} C_j^{(1)} \\ C_j^{(2)} \end{bmatrix} \right]^T \left[\begin{bmatrix} \cos(i\theta) & -\sin(i\theta) \\ \sin(i\theta) & \cos(i\theta) \end{bmatrix} \begin{bmatrix} B_i^{(1)} \\ B_i^{(2)} \end{bmatrix} \right] \\
&= \begin{bmatrix} C_j^{(1)} & C_j^{(2)} \end{bmatrix} \begin{bmatrix} \cos(j\theta) & \sin(j\theta) \\ -\sin(j\theta) & \cos(j\theta) \end{bmatrix} \begin{bmatrix} \cos(i\theta) & -\sin(i\theta) \\ \sin(i\theta) & \cos(i\theta) \end{bmatrix} \begin{bmatrix} B_i^{(1)} \\ B_i^{(2)} \end{bmatrix}
\end{aligned}$$

Expanding the product of the two rotary matrices, we have

$$\begin{bmatrix} \cos(j\theta)\cos(i\theta) + \sin(j\theta)\sin(i\theta) & -\cos(j\theta)\sin(i\theta) + \sin(j\theta)\cos(i\theta) \\ -\sin(j\theta)\cos(i\theta) + \cos(j\theta)\sin(i\theta) & \sin(j\theta)\sin(i\theta) + \cos(j\theta)\cos(i\theta) \end{bmatrix}$$

Finally, we get

$$\langle f_C(x_j, j), f_B(x_i, i) \rangle = \begin{bmatrix} C_j^{(1)} & C_j^{(2)} \end{bmatrix} \begin{bmatrix} \cos((j-i)\theta) & -\sin((j-i)\theta) \\ \sin((j-i)\theta) & \cos((j-i)\theta) \end{bmatrix} \begin{bmatrix} B_i^{(1)} \\ B_i^{(2)} \end{bmatrix}$$

The above derivation is only for the case of word embedding dimension $d = 2$, when $d > 2$, the two-dimensional case can be extended to any dimension as follows

$$f_{\{C,B\}}(x_j, j) = \mathbb{R}_{\Theta,j}^d W_{\{C,B\}} x_j$$

The inner product satisfies linearity, so for any even-dimensional RoPE, we can represent it as a concatenation of the two-dimensional case, that is, grouping the elements of the word embedding vector in pairs

$$\mathbb{R}_{\Theta,j}^d = \begin{bmatrix} \cos j\theta_0 & -\sin j\theta_0 & 0 & 0 & \dots & 0 & 0 \\ \sin j\theta_0 & \cos j\theta_0 & 0 & 0 & \dots & 0 & 0 \\ 0 & 0 & \cos j\theta_1 & -\sin j\theta_1 & \dots & 0 & 0 \\ 0 & 0 & \sin j\theta_1 & \cos j\theta_1 & \dots & 0 & 0 \\ \vdots & \vdots & \vdots & \vdots & \ddots & \vdots & \vdots \\ 0 & 0 & 0 & 0 & \dots & \cos j\theta_{d/2} & -\sin j\theta_{d/2-1} \\ 0 & 0 & 0 & 0 & \dots & \sin j\theta_{d/2} & \cos j\theta_{d/2-1} \end{bmatrix}$$

Each group applies the same rotation operation and the rotation angle of each group is calculated as follows:

$$\Theta = \{\theta_i = 10000^{-2(i-1)/d}, i \in [1, 2, \dots, d/2]\}$$

□

B Implementation Code

B.1 RoPE

Listing 1 PyTorch example of RoPE.

```
class RotaryEmbedding:
    def __init__( self ,dim,max_position_embeddings ,base=10000,scaling_factor=1.0):
        self.dim,self.base,self.max_position_embeddings,self.scaling_factor=dim,
            base,max_position_embeddings,scaling_factor
        inv_freq=1.0/( self.base** ( torch.arange(0,self.dim,2)/self.dim))
        self.register_buffer("inv_freq",inv_freq)

    def forward( self ,x,position_ids):
        seq_len=torch.max(position_ids)+1
        if seq_len > self.max_position_embeddings:
            base=self.base*(( self.scaling_factor*seq_len/self.
                max_position_embeddings)-(self.scaling_factor-1))*( self.dim/( self
                    .dim-2))
            inv_freq=1.0/( base** ( torch.arange(0,self.dim,2)/self.dim))
        else:
            inv_freq = self.inv_freq
        inv_freq_expanded=inv_freq[None,:,:None].expand(position_ids.shape
            [0],-1,1)
        position_ids_expanded=position_ids[:,None,:]
        freqs=(inv_freq_expanded@position_ids_expanded).transpose(1,2)
        emb=torch.cat((freqs,freqs),dim=-1)
        cos,sin=emb.cos().to(x.dtype),emb.sin().to(x.dtype)
        return cos,sin

    def rotate_half(x):
        x1,x2 = x[..., : x.shape[-1] // 2],x[..., x.shape[-1] // 2 :]
        return torch.cat((-x2, x1), dim=-1)

    def apply_QK_rotary_pos_emb(q,k,cos,sin,unsqueeze_dim=2):
        cos,sin = cos.unsqueeze(unsqueeze_dim),sin.unsqueeze(unsqueeze_dim)
        q_embed=(q*cos)+(rotate_half(q)*sin)
        k_embed=(k*cos)+(rotate_half(k)*sin)
        return q_embed,k_embed

    def apply_CB_rotary_pos_emb(c,b,cos,sin,unsqueeze_dim=2):
        cos,sin = cos.unsqueeze(unsqueeze_dim),sin.unsqueeze(unsqueeze_dim)
        c_embed=(c*cos)+(rotate_half(c)*sin)
        b_embed=(b*cos)+(rotate_half(b)*sin)
        return c_embed,b_embed
```

B.2 SSD

Listing 2 Example SSD helper function in PyTorch

```
def pad_tensor_by_size(input_tensor, pad_size):
    # Pad seq_len to be multiple of chunk_len
    return F.pad(input_tensor, (0,0,0,0,0,pad_size,0,0) if len(input_tensor.shape)
        ==4 else (0,0,0,pad_size,0,0))

def reshape_into_chunks(input_tensor, pad_size, chunk_len):
    # Padding input_tensor with `pad_size` on the seq_len dim (dim=1) and
    # simultaneously splitting it into chunk sequences.
    # b t ... -> b (l c) ...
    if len(pad_tensor_by_size(input_tensor, pad_size).shape)==3:
        return rearrange(input_tensor, 'b(lc)h->blch', c=chunk_len)
    else:
        return rearrange(input_tensor, 'b(lc)hd->blchd', c=chunk_len)

def segment_sum(input_tensor):
    # More stable segment sum calculation. Uses cumulative sums and masking
    # instead of direct subtractions.
    chunk_len=input_tensor.size(-1)
    # 1. expand input tensor to have an additional dimension and repeat along
    # that dimension
    # [..., chunk_len] -> [..., chunk_len, chunk_len]
    input_tensor=input_tensor[...,None].expand(*input_tensor.size(), chunk_len)
    # 2. create a lower triangular mask with the diagonal set to 0 to 0 out
    # elements above diag
    mask=torch.tril(torch.ones(chunk_len, chunk_len, device=input_tensor.device,
        dtype=torch.bool), diagonal=-1)
    input_tensor=input_tensor.masked_fill(~mask, 0)
    # 3. compute actual cumsum
    tensor_segsum=torch.cumsum(input_tensor, dim=-2)
    # 4. apply mask to keep only the lower triangular part of the cumulative sum
    # result (incl diagonal this time)
    mask=torch.tril(torch.ones(chunk_len, chunk_len, device=input_tensor.device,
        dtype=torch.bool), diagonal=0)
    tensor_segsum=tensor_segsum.masked_fill(~mask, -torch.inf)
    return tensor_segsum
```

Listing 3 Example SSD algorithm in PyTorch. We have changed some slow methods to faster ones. The original SSD algorithm implementation can be found in the Mamba2 paper.

```

def ssd(x, dt, A, B, C, chunk_len, D):
    seq_len = x.size(1)
    pad_size = (chunk_len - seq_len % chunk_len) % chunk_len
    D_residual = rearrange(D, '... -> ... 1') * pad_tensor_by_size(x, pad_size)
    # Discretize x and A
    x, A = x * rearrange(dt, '... -> ... 1'), A.to(x.dtype) * dt
    # Rearrange into blocks/chunks
    x, A, B, C = [reshape_into_chunks(t, pad_size, chunk_len) for t in (x, A, B, C)]
    # Compute cumulative sum of A
    A = rearrange(A, 'bclh->bhcl', l=chunk_len)
    A_cumsum = torch.cumsum(A, dim=-1)
    # 1. Compute the output for each intra-chunk (diagonal blocks)
    # This is the analog of a causal mask
    L = torch.exp(segment_sum(A))
    # First, contraction of C and B to get G (attention-weights like)
    G = (rearrange(C, 'blchn->blclhn') * rearrange(B, 'blchn->bl1chn')).sum(dim=-1) #
        shape: (b, c, l, s, h)
    # Step 2: Compute M, equivalent to applying attention mask to weights
    M_intermediate = rearrange(G, '... -> ... 1') * rearrange(L, 'bhclst->bcsth1')
    M = M_intermediate.sum(dim=-1)
    # Step 3: Compute Y_diag (apply to values)
    Y_diag = (rearrange(M, '... -> ... 1') * rearrange(x, 'blchp->bl1chp')).sum(3)
    # (right term of low-rank factorization of off-diagonal blocks; B terms)
    decay_states = torch.exp((A_cumsum[:, :, :, -1:] - A_cumsum))
    B_decay_contraction = B * rearrange(decay_states, 'bhcl->bclh1')
    # permute back B * decay states
    states = (rearrange(B_decay_contraction, 'bclhs->bchls1') * rearrange(x, 'blchp->
        blhc1p')).sum(dim=3).permute(0, 1, 2, 4, 3)
    previous_states = torch.zeros_like(states[:, :1])
    states = torch.cat([previous_states, states], dim=1)
    decay_chunk = torch.exp(segment_sum(nn.functional.pad(A_cumsum[:, :, :, -1], (1, 0))
        ))
    states_permuted = states.permute(0, 2, 1, 3, 4)
    result = (decay_chunk[..., None, None] * states_permuted[:, :, :, None, ...]).sum(dim=2)
    new_states = result.permute(0, 2, 1, 3, 4)
    states = new_states[:, :-1]
    # Compute state -> output conversion per chunk
    # (left term of low-rank factorization of off-diagonal blocks; C terms)
    # compute Yoff
    C_times_states = rearrange(C, 'bclhn->bclh1n') * rearrange(states, 'bchpn->bclhpn')
    Y_off = (C_times_states.sum(-1) * rearrange(torch.exp(A_cumsum), 'bhcl->bclh1'))
    # Add output of intra-chunk and inter-chunk terms (diagonal and off-diagonal
        blocks)
    y = rearrange(Y_diag + Y_off, 'bclhp->b(cl)hp') + D_residual
    # Cutting off padded chunks
    if pad_size > 0:
        y = y[:, :seq_len, :, :]

```

Listing 4 Example SSD implementation in PyTorch

```
class SSD(nn.Module):
    def __init__(self, d_model, n_heads, d_head, n_groups, d_state, chunk_len):
        super().__init__()
        self.n_heads, self.n_groups, self.d_state, self.chunk_len = n_heads, n_groups,
            d_state, chunk_len
        # Initialize parameters
        self.X_proj = nn.Linear(d_model, self.n_heads * d_head)
        self.A_log = nn.Parameter(torch.log(torch.arange(1, self.n_heads + 1)))
        self.B_proj = nn.Linear(d_model, self.n_groups * self.d_state)
        self.C_proj = nn.Linear(d_model, self.n_groups * self.d_state)
        self.dt_proj = nn.Linear(d_model, self.n_heads)
        self.D = nn.Parameter(torch.ones(self.n_heads))
        self.out_proj = nn.Linear(d_model, d_model)

    def forward(self, x):
        """
        Notations: b - batch size d - d_model
                   h - n_heads p - d_head n - d_state g - n_groups
                   t - target sequence length s - source sequence length
                   c - n_chunks l - chunk_len
        """
        dtype = x.dtype
        A = -torch.exp(self.A_log.float())
        B = rearrange(self.B_proj(x), 'bt(gn)->btgn', g=self.n_groups, n=self.d_state)
            .repeat(1, 1, self.n_heads // self.n_groups, 1)
        C = rearrange(self.C_proj(x), 'bt(gn)->btgn', g=self.n_groups, n=self.d_state)
            .repeat(1, 1, self.n_heads // self.n_groups, 1)
        dt = self.dt_proj(x)
        x = rearrange(self.X_proj(x), 'bt(hp)->bthp', h=self.n_heads)
        dt = nn.functional.softplus(dt)
        # Apply rotary position embedding to B and C
        cos, sin = self.BC_rotary_emb(hidden_states, position_ids=position_ids)
        C, B = apply_CB_rotary_pos_emb(C, B, cos, sin)
        try:
            y = mamba_chunk_scan_combined(x, dt, A, B, C, chunk_size=self.chunk_len, D=
                self.D)
        except Exception as e:
            y = ssd(x, dt, A, B, C, self.chunk_len, self.D)
        y = self.out_proj(rearrange(y, 'bthp->bt(hp)').to(dtype))
        return y
```

B.3 InnerFuncAttn

Listing 5 Example static attention mask method in PyTorch

```
def static_mask (attention_mask , q_len , kv_len ) :
    """
    notation :
    attention_mask : [bsz , seq_len]
    q_len : query length
    kv_len : key and value length
    """
    bsz , seq_len = attention_mask.size ()
    # Create causal mask
    causal_mask = torch.full ((q_len , kv_len) , float ('-inf')). triu (1)
    # Expand shape
    causal_mask = causal_mask [None , None , : , :]. expand (bsz , 1 , -1 , -1)
    attention_mask = attention_mask [: , None , None , :]. expand (-1 , 1 , 1 , -1)
    # Apply padding
    padding = causal_mask [: , : , : , : seq_len] + attention_mask
    return causal_mask [: , : , : , : seq_len]. masked_fill (padding==0 , float ('-inf'))
```

Listing 6 Example dynamic attention mask method in PyTorch

```
def dynamic_mask (attention_mask , dynamic_mask , q_len , kv_len ) :
    """
    notation :
    attention_mask : [bsz , seq_len]
    dynamic_mask : [n_heads , max_position_len]
    q_len : query length
    kv_len : key and value length
    """
    bsz , seq_len = attention_mask.size ()
    num_heads = dynamic_mask.size (0)
    # Create causal mask
    causal_mask = torch.full ((q_len , kv_len) , float ('-inf')). triu (1)
    # Expand shape
    causal_mask = causal_mask [None , None , : , :]. expand (bsz , num_heads , -1 , -1)
    attention_mask = attention_mask [: , None , None , :]. expand (-1 , num_heads , 1 , -1)
    dynamic_mask = dynamic_mask [None , : , None , : seq_len]. expand (bsz , -1 , 1 , -1)
    # Apply padding
    padding = causal_mask [: , : , : , : seq_len] + attention_mask * dynamic_mask
    return causal_mask [: , : , : , : seq_len]. masked_fill (padding==0 , float ('-inf'))
```

Listing 7 Example InnerFuncAttn implementation in PyTorch

```
class InnerFuncAttn(nn.Module):
    def __init__(self, d_model, n_heads, n_innerV, d_innerV_ret, max_position):
        super().__init__()
        self.n_heads, self.d_head=n_heads, d_model//n_heads
        # Initialize Parameters
        self.Q_proj=Linear(d_model, d_model)
        self.K_proj=Linear(d_model, d_model)
        self.dynamic_mask=Parameter(torch.ones(n_heads, max_position))
        self.V_queries=Linear(d_model, d_innerV_ret)
        self.V_keys=Parameter(torch.zeros(n_innerV, d_innerV_ret))
        self.V_embed=Embedding(n_heads, d_model)
        self.out_proj=Linear(d_model, d_model)
        # Rotary Position Embedding
        self.QK_rotary_emb=RotaryEmbedding(self.d_head, max_position)

    def inner_func(self, x):
        V_queries=self.V_queries(x)
        sim=torch.matmul(V_queries, self.V_keys.T) # einsum('btn, kn->btk')
        V_embed=self.V_embed(sim.topk(1, dim=-1).indices)
        V=x*V_embed.sum(dim=-2) # einsum('btd, btkd->btd')
        return V

    def forward(self, x, attention_mask, position_ids):
        """
        Notation: b - batch t - length d - d_model h - n_heads p - d_head
        """
        # Compute linear projection Q K and inner function V
        Q=self.Q_proj(x)
        K=self.K_proj(x)
        V=self.inner_func(x)
        # Split into multiple heads
        Q, q_len=rearrange(Q, "bt (hp)->bhttp", h=self.n_heads), Q.size(1)
        K, kv_len=rearrange(K, "bt (hp)->bhttp", h=self.n_heads), K.size(1)
        V=rearrange(V, "bt (hp)->bhttp", h=self.n_heads)
        # Apply rotary position embedding to Q and K
        cos, sin=self.QK_rotary_emb(V, position_ids=position_ids)
        Q,K=apply_QK_rotary_pos_emb(Q,K, cos, sin)
        # Compute Attention score matrix and rotary position embedding matrix
        attn_score=torch.matmul(Q,K.transpose(-2,-1))/math.sqrt(self.d_head)
        mask=dynamic_mask(attention_mask, self.dynamic_mask, q_len, kv_len)
        attn_score=attn_score+mask
        attn_score=F.softmax(attn_score, dim=-1)
        # Weighted attention score to inner function state V
        y=torch.matmul(attn_score, V)
        y=rearrange(y, "bhttp->bt (hp)")
        # Project Output
        y=self.out_proj(y)
        return y
```

B.4 Cross Domain Mixture of Experts

Listing 8 Example CDMoE implementation in PyTorch

```
class CDMoE(nn.Module):
    def __init__(self, d_model, act, d_ff, d_ret, n_experts, n_heads, k_per_head):
        super().__init__()
        self.act_fn, self.n_heads, self.k_per_head = ACT2FN[act], n_heads, k_per_head
        # Cross Domain
        self.shared_up_proj = Linear(d_model, d_ff)
        self.shared_down_proj = Linear(d_ff, d_ff_private)
        # Queries and Keys
        self.queries = Linear(d_model, d_ret * n_heads)
        self.num_keys = math.sqrt(n_experts)
        self.keys = Parameter(torch.zeros(n_heads, self.num_keys, 2, d_ret // 2))
        # Private Experts
        self.down_embed = Embedding(n_experts, d_model)
        self.up_embed = Embedding(n_experts, d_model)

    def forward(self, x):
        """
        Notation: b - batch t - length d - d_model n - d_retrieval
                  h - n_heads p - 2 for product key k - number of keys
        """
        # Compute Cross Domain
        phi_x = self.shared_down_proj(self.act_fn(self.shared_up_proj(x)))
        # Queries and Keys for Product-Key
        queries = self.queries(phi_x)
        queries = rearrange(queries, 'bt(phn)->pbthn', p=2, h=self.n_heads)
        # Compute scores and indices
        sim = einsum('pbthn, hkpn->pbthk', queries, self.keys)
        (s_x, s_y), (i_x, i_y) = sim.topk(self.k_per_head, dim=-1)
        all_s = einx.add('..._i, ..._j -> ..._(i_j)', s_x, s_y)
        all_i = einx.add('..._i, ..._j -> ..._(i_j)', i_x * self.num_keys, i_y)
        s, pk_i = all_s.topk(self.k_per_head, dim=-1)
        i = all_i.gather(-1, pk_i)
        # Compute Private Experts
        down_embed, up_embed = self.down_embed(i), self.up_embed(i)
        experts_s = self.act_fn(einsum('btd, bthkd->bthk', phi_x, down_embed) * s)
        y = einsum('bthk, bthkd->btd', experts_s, up_embed) + phi_x
        return y
```

C Evaluation Parameters

C.1 Multi-Query Associative Recall

Table 5: **Data Parameters.** We introduce a more challenging task version based on the original multi-query associative recall (Arora et al. 2024), where tokens that are not query/key/value are replaced with random tokens. We also use more key-value pairs and longer sequence lengths. For each sequence length $T \in \{256, 512, 1024, 2048\}$, we use $T/4$ key-value pairs. The total vocabulary size is 8192, with approximately 250k training samples and 1k test samples.

VOCAB	SEQ LEN	KV PAIRS	TRAIN EXAMPLES	TEST EXAMPLES	POW A	BATCH	MAX EPOCHS
8192	256	64	2^{18}	2^{10}	0.01	256	64
8192	512	128	2^{18}	2^{10}	0.01	128	64
8192	1024	256	2^{18}	2^{10}	0.01	64	64
8192	2048	512	2^{18}	2^{10}	0.01	32	64

Table 6: **Model Parameters.** These algorithms can all split into multiple heads, so we set them to single heads and use common single head dimensions $d_{model} \in \{32, 64, 128, 256\}$. For fairness, the SSD algorithm is different from the validation structure in Mamba2 (Dao and Gu 2024) and we remove the one-dimensional causal convolution and gated MLP. All algorithms use the structure of sequence transformation to state transformation and stack 2 layers. In preparation for subsequent algorithm mixing, the learning rate for each dimension of these algorithms is the same.

ALGORITHM	d_{model}	n_{layers}	n_{heads}	d_{state}	chunk_len	n_v	d_{innerV}	LEARNING RATE
QCAtn	32/64/128/256	2	1	—	—	—	—	4e-4/3e-4/2e-4/1e-4
SSD	32/64/128/256	2	1	128	256	—	—	4e-4/3e-4/2e-4/1e-4
InnerFuncAttn	32/64/128/256	2	1	—	—	2	16/32/64/128	4e-4/3e-4/2e-4/1e-4

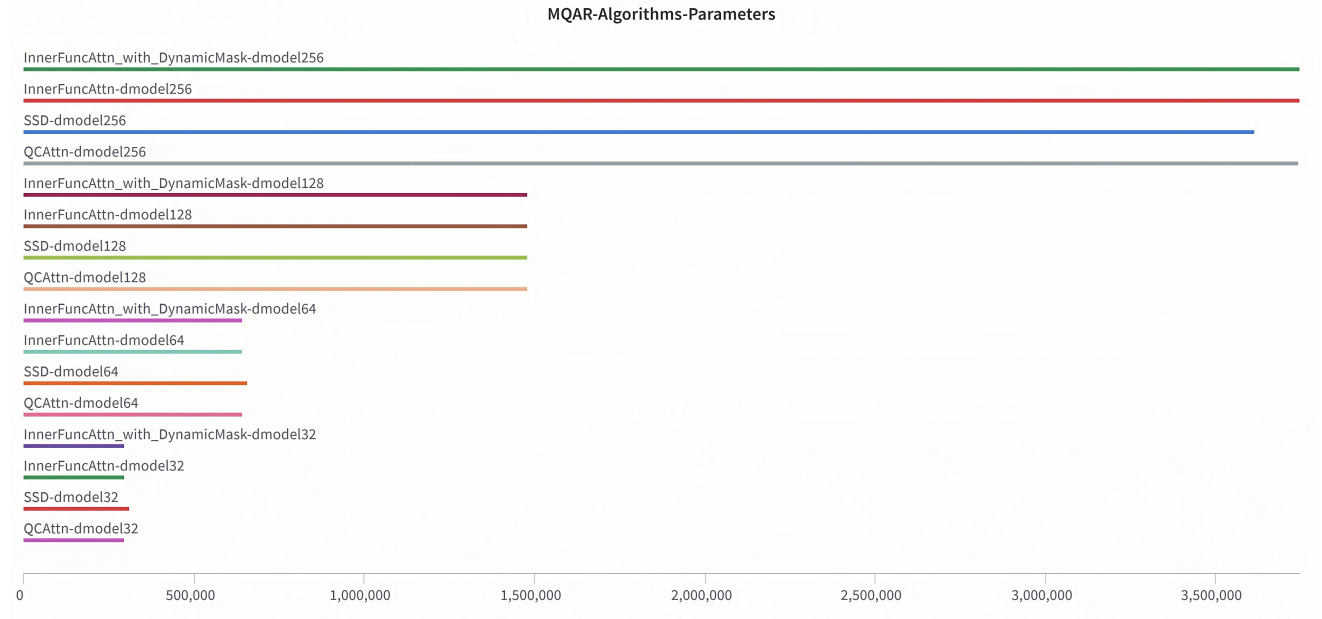


Figure 8: **Different Algorithms Parameters.** Whether adding dynamic attention mask or not, the number of parameters of InnerFuncAttn is similar to QCAtn at different dimensional scales. SSD increases the number of parameters less when increasing the dimensional scale.

C.2 Downstream Evaluation

To avoid score bias in downstream tasks due to different training data, we retrain four model architectures, including Llama using the QCAttn algorithm, Mamba2 using the SSD algorithm, Jamba using the hybrid of QCAttn and SSD, and our architecture. We train models of two scales, 360M and 1.3B, with parameters referenced in the table7.

- All models are trained on the Smollm-Corpus (Ben Allal et al. 2024) dataset using the NeoX tokenizer.
- The training environment is the Nvidia open-source PyTorch image (NVIDIA 2022) version 24.2, which is compatible with the cuda kernel SSD algorithm in the mamba-ssm library.
- Training is completed using the Trainer class in the Transformers (Wolf et al. 2020) library.
- AdamW optimizer hyperparameters $\beta_1 = 0.9$, $\beta_2 = 0.999$ and $weight_decay = 0.01$.
- The linear warm-up steps are 10% of the total steps, reaching the maximum learning rate of $2e - 4$, and then cosine decay to the minimum learning rate of $2e - 5$.
- No bias terms.
- RMSNorm instead of LayerNorm.

For downstream evaluation, we use LM evaluation harness from EleutherAI (L. Gao et al. 2021), the validation dataset includes the following tasks:

- MMLU (Hendrycks et al. 2021)
- TriviaQA (Joshi et al. 2017)
- ARC (Clark et al. 2018)
- PIQA (Bisk et al. 2020)
- HellaSwag (Zellers et al. 2019)
- OBQA (Mihaylov et al. 2018)
- Winogrande (Sakaguchi et al. 2021)

Table 7: **Model Parameters.** For fairness, we adjust the important parameters of these four models to be as close in size as possible, and ensure that the total parameters and activation parameters of the four models are as close as possible by adding routing mixture of experts in LLaMa and Mamba2, and carefully adjusting the feedforward network expansion size of LLaMa, Mamba2, and Jamba. Finally, we obtain models of two scales, 320M and 1.3B.

MODEL	d_{model}	n_{layers}	n_{heads}	d_{state}	chunk_len	n_v	$n_{experts}$	LEANING RATE	BATCH SIZE
LlaMa-320M	768	24	12	—	—	—	4	3e-4	1M tokens
Mamba2-320M	768	24	12	128	256	—	4	3e-4	1M tokens
Jamba-320M	768	24	12	128	256	—	4	3e-4	1M tokens
Cheems-320M	768	24	12	128	256	6	3072	3e-4	1M tokens
LlaMa-1.3B	2048	24	32	—	—	—	4	2e-4	2M tokens
Mamba2-1.3B	2048	24	32	128	256	—	4	2e-4	2M tokens
Jamba-1.3B	2048	24	32	128	256	—	4	2e-4	2M tokens
Cheems-1.3B	2048	24	32	128	256	16	8192	2e-4	2M tokens